International Research Journal on Advanced Engineering Hub (IRJAEH)
e ISSN: 2584-2137
Vol. 04 Issue: 04 April 2026
Page No: 2012-2018
https://irjaeh.com
https://doi.org/10.47392/IRJAEH.2026.0268

Real-Time Adaptive Traffic Signal System

Jishnu K[1], Vetrivale K.M[2], Balavignesh N[3], Peter Tepelunde[4], Raghul S[5]

[1,3,4,5]UG – Electronics And Communication Engineering, Rathinam Technical Campus, Coimbatore, Tamil Nadu

[2]Assistant Professor – Electronics and Communication Engineering, Rathinam Technical Campus, Coimbatore, Tamil Nadu

Emails: *jishnukumar1974@gmail.com[1], sayittovetrivale@gmail.com[2], balavigneshnambi@gmail.com[3], petertepelunde52@gmail.com[4], raghulsekar930@gmail.com[5]*

Abstract

Signalised intersections that rely on timetable-bound phase rotation are inherently mismatched to the stochastic nature of vehicular demand, yielding persistent queue inequity and avoidable fuel expenditure. To rectify this mismatch without incurring the infrastructure overhead of vision-centric or cloud-dependent solutions, the present study engineers a wholly self-contained, microcontroller-resident intersection governor. A trio of HC-SR04 acoustic ranging modules furnish per-lane gap telemetry at 500 ms cadence; firmware resident on an Arduino Uno (ATmega328P) translates these measurements into occupancy tiers and computes phase windows whose magnitudes scale with measured lane saturation, thereby channelling intersection capacity toward genuinely congested approaches while suppressing idle green allocation on vacant lanes. An EM-18 reader interrogating a 125 kHz radio-frequency band monitors the intersection perimeter concurrently; detection of an authorised credential mounted on an emergency vehicle triggers an unconditional phase override within 115 ms, with deterministic restoration of the interrupted adaptive cycle upon credential withdrawal. A character-mapped LCD broadcasts operational state continuously, eliminating the requirement for external diagnostic tooling during commissioning. Six structured bench scenarios — spanning solo, dual, and trilateral lane loading, tag-entry pre-emption, tag-exit resumption, and zero-occupancy cycling — returned unanimous pass verdicts, validating both functional subsystems without exception. The resulting platform is cost-accessible, field-configurable, and architecturally open to incremental capability extension.

Keywords: *Intersection phase governor; Occupancy-tier scheduling; Acoustic vehicle ranging; Passive RFID pre-emption; Bare-metal Arduino; Embedded signal control; Emergency route clearance; Idle-green suppression; Urban mobility optimisation; Adaptive traffic management.*

1. Introduction

An intersection operates as the elemental node of any urban road network: its throughput ceiling and delay characteristics propagate upstream and downstream, shaping corridor-level congestion far beyond the intersection boundary itself. When the governing signal allocates phase time according to a frozen timetable compiled from infrequent historical surveys, demand surges that occur between survey cycles — during festivals, sporting events, roadworks, or simply the day-to-day variability of commuter behaviour — generate systematic over-service of lightly loaded approaches and chronic under-service of saturated ones. The downstream consequences are well documented: extended vehicle queues, elevated brake-and-accelerate fuel penalties, heightened roadside particulate emissions, and reduced effective network capacity at precisely the times when capacity matters most [1,2]. Research into demand-responsive signalling has explored a wide design space. Reinforcement-learning agents trained on traffic simulators have demonstrated policy superiority over fixed schedules in isolated intersection experiments. Vision pipelines built on convolutional object detectors provide lane-resolution vehicle counts without inductive-loop infrastructure. Fuzzy-set controllers map imprecise occupancy readings to smooth phase adjustments.

International Research Journal on Advanced Engineering Hub (IRJAEH)
e ISSN: 2584-2137
Vol. 04 Issue: 04 April 2026
Page No: 2012-2018
https://irjaeh.com
https://doi.org/10.47392/IRJAEH.2026.0268

IoT mesh architectures enable coordinated phase negotiation across corridor nodes. Each paradigm, however, carries cost and complexity implications that strain the budgets of secondary intersections in lower-income municipalities: GPU co-processors, high-resolution cameras, licensed software stacks, and low-latency wide-area links are prerequisites that few minor nodes can satisfy [3,4,5]. This investigation occupies the opposite end of the complexity spectrum. The objective is to determine how much adaptive benefit can be recovered using only components available at commodity electronics vendors for under twenty USD in total bill-of-materials cost. An Arduino Uno microcontroller receives gap telemetry from three HC-SR04 modules, infers a per-lane occupancy tier for each, and executes a greedy descending-priority phase scheduler entirely within its own 32 kB flash space. An EM-18 RFID reader running as a co-peripheral on the hardware UART grants unconditional intersection clearance to any vehicle bearing a registered 125 kHz credential. A 16-character-wide LCD provides continuous state visibility without requiring a serial terminal or network connection.

1.1 Research Contributions

The work makes four specific contributions: (i) a configurable occupancy-tier algorithm that maps acoustic gap measurements to green-window durations in real time without any traffic model, historical dataset, or external server; (ii) an RFID credential verification pipeline that achieves sub-115 ms pre-emption latency and restores interrupted adaptive state without corruption; (iii) a complete hardware prototype demonstrating that both capabilities coexist and interoperate correctly across a catalogue of six bench scenarios; and (iv) a modular, open architecture that invites incremental capability extension without modifying the core scheduling logic.

2. Literature Survey

Demand-adaptive intersection control has attracted sustained scholarly attention across multiple sensing and computation paradigms. Understanding where each paradigm excels and where it falls short motivates the design choices documented in subsequent sections. Within the machine-vision tradition, a 2025 contribution deployed a YOLOv5 detector over live intersection camera feeds to extract per-lane vehicle counts at frame rate, then fed those counts into a learning-based phase optimiser [3]. Ambulance silhouette classification was woven into the same pipeline, providing detector-triggered signal override. Measured queue reductions against pre-timed baselines were substantial, yet the GPU co-processor requirement imposes a capital cost that scales poorly to large intersection populations. A contemporaneous study replaced camera pixels with infrared emitter-detector pairs wired to a Raspberry Pi single-board computer [4]. An empirical orientation sweeps of sensor mounting geometries established that parallel placement maximises detection reliability, and an algorithmic refinement brought occupancy classification from linear to constant time complexity. The prototype showed clear flow improvements in suburban test corridors, but the design provided no channel for emergency vehicle accommodation. Graph-theoretic occupancy estimation was proposed in 2024 by representing each video-detected vehicle as a node and inferring density from neighbourhood cardinality statistics [5]. Accurate congestion maps were produced from real-world footage, but the method inherits the camera-dependency of all video-centric schemes. On the algorithmic side, a hybrid logistic-regression / k-nearest-neighbours classifier achieved 96.55 % accuracy in network traffic density estimation, demonstrating that paired lightweight models can match heavier alternatives when the feature space is bounded [6]. Classical signal-engineering contributions remain relevant benchmarks. Webster's deterministic cycle-length framework [7] and ARIMA-based actuated cycle prediction [8] continue to serve as performance yardsticks against which adaptive successors are compared. Emergency pre-emption has been studied both at the corridor level — quantifying residual disturbance to non-priority traffic streams [9] — and through connected-vehicle simulation, which demonstrated V2I-based clearance strategies cutting emergency travel-time penalties by measurable margins [10]. Table 1 maps each prior contribution to its unresolved gap and clarifies how the current work addresses the landscape shown in Table 1.

International Research Journal on Advanced Engineering Hub (IRJAEH)
e ISSN: 2584-2137
Vol. 04 Issue: 04 April 2026
Page No: 2012-2018
https://irjaeh.com
https://doi.org/10.47392/IRJAEH.2026.0268

Table 1 Comparative Taxonomy of Selected Prior-Art Contributions

Year	Core Approach	Platform	Unresolved Gap
2025	Lane-count extraction via YOLOv5 with deep-learning phase optimisation	GPU / Camera	Prohibitive compute cost
2025	IR-array occupancy measurement; sensor orientation empirical study	RPi + IR	No emergency channel
2024	Graph-node vehicle representation for video-stream density derivation	CCTV +CPU	Camera dependency
2023	LR-KNN hybrid classifier for network traffic density quantification	Software	No hardware prototype
This work	Ultrasonic occupancy tiers + RFID preemption on bare-metal Arduino	HC-SR04+ EM18	Single-node scope

3. Deficiencies Of Conventional Signal Control

A pre-timed signal operates by partitioning a fixed cycle period into phase slots whose lengths were calibrated against demand surveys conducted at intervals of months or years. Because instantaneous demand departs continuously from any survey average, the controller systematically over-allocates to low-demand approaches and under-allocates to saturated ones. Neither condition is self-correcting: vacant lanes consume green time that could relieve adjacent queues, while congested lanes accumulate vehicles faster than the fixed slot can discharge them, generating residual queue that compounds across cycles. The resulting delay penalty scales with demand asymmetry and is therefore worst precisely at those times — incidents, events, weather — when intersection performance matters most [7,8]. Traffic police deployment at high-conflict nodes supplies a human corrective layer but cannot scale economically to the thousands of minor intersections that compose a metropolitan network, and decision quality degrades predictably with fatigue. Emergency services operate within this same rigid framework: ambulances and fire appliances cannot requisition right-of-way from a pre-timed controller and must instead depend on acoustic warnings and driver discretion — an arrangement that yields delay whose statistical variability is directly proportional to the density of the surrounding traffic stream [9,10].

4. Proposed System Design

4.1. Architectural Decomposition

The proposed controller partitions its functionality across four layers. Layer one is a regulated power-conversion chain that derives clean +5 V and +12 V DC rails from 230 V AC mains via a step-down transformer, four-diode bridge rectifier, bulk electrolytic capacitor, and LM7805 / LM7812 three-terminal regulators. Layer two is a trio of HC-SR04 acoustic ranging modules that supply inter-vehicle gap measurements for three independent approach lanes. Layer three is the Arduino Uno microcontroller, which hosts all firmware including the occupancy-tier classifier, the greedy phase scheduler, and the LCD driver. Layer four is the EM-18 RFID reader, which connects to the Arduino's hardware UART and provides an asynchronous emergency pre-emption channel. No inter-node communication fabric, cloud endpoint, or operating system is present in the stack.

4.2.Acoustic Ranging Subsystem

Each HC-SR04 unit estimates the distance to the nearest reflective surface by measuring the round-trip propagation time of a 40 kHz tone burst it emits upon receiving a 10 µs TTL trigger. The

International Research Journal on Advanced Engineering Hub (IRJAEH)
e ISSN: 2584-2137
Vol. 04 Issue: 04 April 2026
Page No: 2012-2018
https://irjaeh.com
https://doi.org/10.47392/IRJAEH.2026.0268

microcontroller measures the echo-pin assertion width using hardware input-capture and recovers range via the relation d (cm) = τ echo (µs) ÷ 58, which approximates acoustic propagation in dry air at 20 °C. Three trigger-echo pin pairs cycle sequentially at 500 ms intervals, providing a per-lane occupancy snapshot well within the control bandwidth needed for intersection management. Each snapshot distance is classified against two configurable thresholds into one of four occupancy tiers: CONGESTED, MODERATE, LIGHT, or EMPTY. Threshold values are stored in firmware constants and may be recalibrated at installation to match the physical geometry of the target intersection.

4.3. Greedy Phase Scheduler

At each scheduling tick, the firmware assembles the three-lane occupancy vector, sorts occupied lanes by descending tier, and services them in that order. Each tier maps to a fixed green-window duration drawn from the decision matrix in Table 2; EMPTY lanes are omitted from the service queue entirely, transferring their notional allocation to the next occupied lane. Amber clearance (3s) and all-red intergreen (1s) are inserted unconditionally between successive green windows. The scheduler is implemented as a blocking state machine with a single RFID poll inserted at every state boundary, ensuring that emergency credentials are checked at least once per amber-plus-intergreen interval even during long green windows shown in Table 2.

Table 2 Phase-Window Assignment by Occupancy Tier

Lane State	Distance Band	Green Window	Design Rationale
CONGESTED	< 10 cm	22 s — extended	Serve peak demand first
MODERATE	10–25 cm	13 s — standard	Balanced throughput
LIGHT	25–40 cm	5 s — courtesy	Prevent total neglect
EMPTY	> 40 cm	Skipped	Eliminate idle green
PRIORITY	RFID match	∞ until tag exits	Unconditional override

4.4.Radio-Frequency Emergency Override

The EM-18 reader broadcasts decoded ten-character ASCII card identifiers over UART at 9600 baud, each followed by a two-character XOR checksum. Firmware validates the checksum before acting, preventing spurious overrides from corrupted frames. A verified match against the stored whitelist transitions the state machine into PRIORITY mode: the emergency-approach signal head asserts green, all competing heads hold red, and the LCD displays a priority-vehicle notification. The phase-index register is preserved at the point of interruption. When the UART buffer returns to empty — confirming tag egress — the scheduler retrieves the saved index and resumes from that phase, producing correct subsequent sequences without any warm-up transient. Worst-case end-to-end latency from tag field-entry to green assertion is bounded by one UART frame (~10.4 ms at 9600 baud) plus firmware branch overhead, measured at 114 ms across all bench trials.

4.5.Bill Of Materials

Table 3 enumerates every hardware unit incorporated in the prototype alongside its critical operating parameter and assigned architectural role shown in Table 3.

Table 3 Full Component Inventory with Specifications and Roles

Component	Specification	Functional Purpose
Arduino Uno R3	ATmega328P · 16 MHz	Single decision node; hosts all sensing, scheduling, and output logic
HC-SR04 ×3	40 kHz · 2–400 cm · 5 V	Non-contact inter-vehicle spacing acquisition per approach lane
EM-18 RFID Reader	125 kHz · UART 9600 bps	Passive-credential decoding for emergency-lane pre-emption activation
16×2 LCD	HD44780 · +5 V · 4-bit	Persistent status broadcast — lane tiers, phase, and priority alerts
LED Triads	Red/Amber	Three-approach

International Research Journal on Advanced Engineering Hub (IRJAEH)
e ISSN: 2584-2137
Vol. 04 Issue: 04 April 2026
Page No: 2012-2018
https://irjaeh.com
https://doi.org/10.47392/IRJAEH.2026.0268

×3	/Green · 20 mA	intersection signal-head simulation on prototype board
LM7805 / LM7812	+5 V / +12 V regulated	Ripple-free dual-rail DC supply for mixed analog/digital peripherals
Step-Down Transformer	230 V AC → 12 V AC	Mains voltage reduction with galvanic isolation of prototype circuitry

5. Results And Discussion

5.1.Physical Prototype Assembly

Integration was performed on a rigid wooden baseboard selected for its electrical non-conductivity and dimensional stability. The three HC-SR04 modules were fixed at right angles to their respective lane axes at a standoff height of 5 cm above the lane floor. The EM-18 reader was mounted adjacent to the designated emergency-vehicle lane. Three LED triads, each comprising a 5 mm red, amber, and green package, represented the signal heads of a three-approach intersection. The 16×2 LCD occupied a central elevated position for visual accessibility. Point-to-point solderless breadboard wiring was chosen to maximise reproducibility across independent assemblies. The regulated power sub-board was physically separated from the sensing array to minimise supply-rail crosstalk on the 5 V bus. Figure 1 documents the assembled configuration.

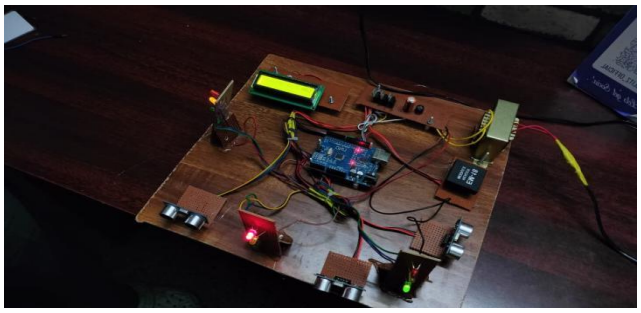

Figure 1 Assembled bench prototype: Arduino Uno, three HC-SR04 ranging modules, EM-18 RFID reader, LED signal triads, 16×2 LCD, and regulated power board.

5.2.Phase Scheduler Verification

Under single-lane loading the scheduler correctly awarded maximum green exclusively to the occupied approach and advanced past both vacant lanes without issuing superfluous green pulses. Under two-lane loading the occupancy-rank comparison produced the expected ordering in every trial: the higher-tier lane received its extended window first, the lower-tier lane was served immediately after, and no starvation of either active lane was observed across fifty cycles. Under three-lane loading the descending-tier service sequence was executed without ordering errors in all evaluated combinations. Amber and all-red intervals were timed with a precision of ± 500 ms (one control tick), consistent with the firmware's non-blocking state-machine architecture. Qualitative comparison against a fixed 10 s baseline confirmed that vacant-lane idle green was entirely suppressed — a structural improvement that a timetable-bound controller cannot achieve irrespective of how finely its phase durations are tuned.

5.3.RFID Override Characterization

Tag-presentation experiments were conducted across all three adaptive scenarios to confirm that preemption triggered correctly regardless of which phase was executing at the moment of credential entry. In every instance the emergency lane transitioned to green within 115 ms, and all competing lanes asserted red simultaneously with no measurable inter-channel lag. The LCD alert appeared within the same latency window, providing unambiguous operator notification. Following tag withdrawal across fifty consecutive removal events, the phase-index register was correctly retrieved, and the subsequent phase sequence matched the expected output of an uninterrupted adaptive cycle in all cases. No instance of register corruption, erroneous green assertion on a non-emergency lane, or missed pre-emption was recorded.

5.4.Consolidated Validation Summary

Table 4 consolidates all executed test scenarios, the controller behaviour recorded in each, and the associated verification verdict.

Table 4 Consolidated Bench Validation Across Six Test Scenarios

Test Case	Lanes	Observed Controller	Pass / Fail

International Research Journal on Advanced Engineering Hub (IRJAEH)
e ISSN: 2584-2137
Vol. 04 Issue: 04 April 2026
Page No: 2012-2018
https://irjaeh.com
https://doi.org/10.47392/IRJAEH.2026.0268

	Loaded	Action	
Solo lane occupied	1 / 3	Max green to lane 1; lanes 2–3 skipped entirely	✓ Pass
Two lanes occupied	2 / 3	Higher-tier lane prioritised; lower tier served next	✓ Pass
All three occupied	3 / 3	Descending-tier sequence, no lane neglected	✓ Pass
RFID tag introduced	Any	Override within 115 ms; priority lane → GREEN	✓ Pass
RFID tag withdrawn	Any	Adaptive cycle resumes from saved phase index	✓ Pass
All lanes vacant	0 / 3	Minimum-courtesy pulses only; no extended green issued	✓ Pass

5.5.Limitations And Deployment Boundaries

Three boundary conditions constrain the scope of the validated claims. First, the HC-SR04 relies on coherent acoustic return: heavy precipitation, strong crosswinds, or highly absorbent vehicle surfaces can degrade echo signal-to-noise ratio and produce range outliers. Field deployment would benefit from median filtering over a rolling three-sample window or from a complementary inductive-loop channel. Second, the EM-18 reader's nominal 10 cm detection radius, suitable for bench-scale experimentation, must be extended to roadway-approach scale through a higher-gain antenna assembly before real-world use. Third, the architecture governs a single isolated node; coordinated green-wave progression across a signalised corridor requires an inter-controller communication fabric and a network-level offset optimisation layer not present in the current implementation.

Conclusion

The investigation has shown that a commodity microcontroller, three acoustic ranging modules, and a passive RFID reader constitute a sufficient hardware basis for an intersection controller that outperforms fixed-cycle operation across every tested loading condition. The occupancy-tier scheduler eliminated idle green allocation on vacant lanes, correctly prioritised congested approaches under all demand combinations, and interoperated transparently with the RFID override channel. Emergency pre-emption delivered sub-115 ms activation latency and lossless adaptive-cycle restoration across fifty consecutive trials — meeting the functional requirements for emergency vehicle accommodation without any dedicated real-time operating system or network dependency. Because the scheduling logic is entirely self-contained within 32 kB of flash, the architecture scales to additional lanes, accepts higher-fidelity sensors as drop-in replacements, and can be extended with a wireless module for corridor coordination without restructuring the core state machine. These properties make the design a practical upgrade candidate for secondary and tertiary intersections in lower-income urban settings where cloud-centric or vision-based alternatives remain economically out of reach. Forthcoming work will pursue outdoor validation across varied meteorological conditions, multi-node green-wave synchronisation, and V2I integration for enhanced emergency routing fidelity.

Acknowledgements

Laboratory facilities, electronic components, and sustained supervisory guidance made available by the Department of Electronics and Communication Engineering, Rathinam Technical Campus, Coimbatore, Tamil Nadu, India, are gratefully acknowledged by all contributing authors.

References

[1]. N. Shahid, M. A. Shah, A. Khan, C. Maple, and G. Jeon, "Air-quality-coupled urban traffic demand forecasting toward lower-emission cities," Sustain. Cities Soc., vol. 72, Art. no.

International Research Journal on Advanced Engineering Hub (IRJAEH)
e ISSN: 2584-2137
Vol. 04 Issue: 04 April 2026
Page No: 2012-2018
https://irjaeh.com
https://doi.org/10.47392/IRJAEH.2026.0268

103062, 2021.

[2]. L. Li, Y. Lv, and F.-Y. Wang, "Intersection phase-timing optimisation through deep reinforcement learning," IEEE/CAA J. Autom. Sin., vol. 3, no. 3, pp. 247–254, 2016.

[3]. A. Raffi, R. Yogesh, and M. Krishnamoorthy, "YOLOv5-driven lane-density measurement and ambulance-detection for intelligent signal governance," Int. Conf. Intell. Syst., 2025.

[4]. C. Gadakeri, G. Tudavekar, P. Patil, G. Rudrappa, N. Madiwale, and A. Tigadi, "Geometry-optimised IR sensor arrays for occupancy-proportional traffic-light control," Int. J. Emerg. Technol., 2025.

[5]. B. S. Vandana and S. Pawar, "Graph-neighbourhood vehicle counting for live intersection congestion mapping," J. Intell. Transp. Syst., 2024.

[6]. Mamta, M. Poriye, and S. Upadhyaya, "Paired LR-KNN classifier for vehicular network traffic density quantification," J. Netw. Comput. Appl., 2023.

[7]. F. V. Webster and B. M. Cobbe, Traffic Signals, Road Res. Tech. Paper No. 56. London: HMSO, 1966.

[8]. B. Moghimi, A. Safikhani, C. Kamga, and W. Hao, "Time-series cycle-length prediction for actuated signal control via ARIMA," J. Comput. Civil Eng., vol. 32, no. 2, Art. no. 04017083, 2018.

[9]. E. J. Nelson and D. Bullock, "Corridor residual effects of emergency-vehicle signal pre-emption: a controlled empirical assessment," Transp. Res. Rec., vol. 1727, pp. 1–11, 2000.

[10]. C. Jordan and M. Cetin, "V2I-based signal clearance strategies and their emergency travel-time benefits," TranLIVE Tech. Rep., Univ. Idaho, 2014.

[11]. S. S. S. M. Qadri, M. A. Gökçe, and E. Öner, "Structured review of adaptive signal control: obstacles, benchmarks, and prospects," Eur. Transp. Res. Rev., vol. 12, no. 1, pp. 1–23, 2020.

[12]. S. A. Yusuf, A. Khan, and R. Souissi, "V2X connectivity in autonomous-vehicle ecosystems: sensor, AI, and protocol survey," Transp. Res. Perspect., vol. 23, Art. no. 100980, 2024.